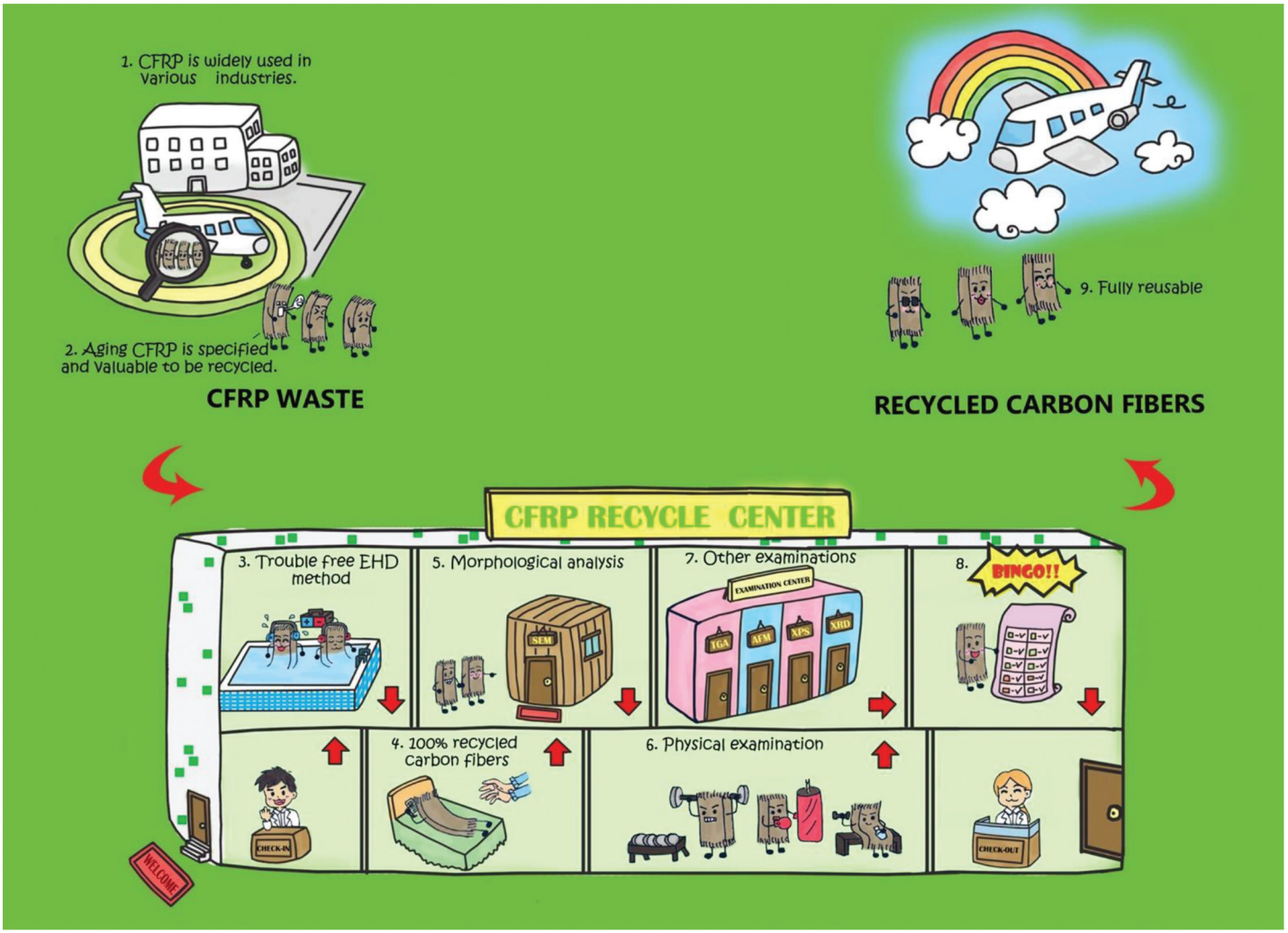

Showcasing Research presented by Prof. Ji-hua Zhu *et al.* of Shenzhen University, P. R. China.

Recycling of carbon fibre reinforced plastics by electrically driven heterogeneous catalytic degradation of epoxy resin

A new recycling technology with the benefit of the electrochemical promotion of the catalysis effect, termed the electrically driven heterocatalytic decomposition (EHD) method, is developed. The simplicity of the procedure and the moderate requirements of the processing facilities remove the CFRP waste size limit, significantly improving the commercial value of the recycled fibres and enabling large-scale implementation.

As featured in:

See Feng Xing *et al.*, *Green Chem.*, 2019, **21**, 1635.

ROYAL SOCIETY OF CHEMISTRY | Celebrating IYPT 2019

rsc.li/greenchem

Registered charity number: 207890

Green Chemistry

PAPER

View Article Online
View Journal | View Issue

Cite this: *Green Chem.*, 2019, **21**, 1635

Recycling of carbon fibre reinforced plastics by electrically driven heterogeneous catalytic degradation of epoxy resin†

Ji-Hua Zhu, [a] Pi-yu Chen,[a] Mei-ni Su, [a,b] Chun Pei[a] and Feng Xing*[a]

The abundant end-of-service-life carbon fibre reinforced plastic (CFRP) composites have become an increasingly significant environmental issue, making the key challenge to be how to increase the resource efficiency by turning waste into reusable materials. Existing recycling technologies generally require complicated processes, expensive facilities or toxic chemicals. Moreover, these demanding conditions limit the size of CFRP waste, resulting in greatly reduced commercial value of recycled fibres and less cost-effective applications. Here, we demonstrate a new recycling technology with the benefit of the electrochemical promotion of the catalysis effect, termed the electrically driven heterocatalytic decomposition (EHD) method. Our results show that even by using simple equipment and conventional nontoxic electrolyte components, intact carbon fibres can be efficiently recycled under atmospheric pressure and at room temperature. The residual strength of the reclaimed carbon fibres (rCFs) is close to that of the virgin carbon fibres (VCFs), i.e., a 90% residual tensile strength and 121% residual interfacial shear strength compared with the VCFs. More importantly, the simplicity of the procedure and the moderate requirements of the processing facilities removal of the CFRP waste size limit, significantly improving the commercial value of the recycled fibres and enabling large-scale implementation.

Received 23rd November 2018,
Accepted 10th February 2019

DOI: 10.1039/c8gc03672a

rsc.li/greenchem

Introduction

CFRPs are composite engineered materials consisting of carbon fibres (CFs) as reinforcements and an organic epoxy resin as a matrix, a combination that renders the materials extremely strong but also lightweight. These features, along with their unique electrical conductivity, thermal stability, good resistance to corrosion, and high rigidity,[1] have led to CFRPs being widely used in the aerospace, vehicle, wind power generation, and construction industries[2,3] since the 1970s. In 2017, the worldwide demand for CFs was 82 400 tons, and this demand is expected to reach 112 000 tons in 2020. Since the service life of CFRPs is approximately 50 years, the extensive use of CFRP is now starting to produce serious waste disposal problems.

Although the CFRP materials reach the end of their service life, the CFs themselves generally retain their properties;[4] therefore, the prospect of recycling CFRP composites without damaging the mechanical properties and dimensions of CFs is of great commercial interest. The recovery value of epoxy resin is not comparable to that of CFs; thus, in recent years, a great number of studies have been conducted on the reclamation of CFs from composite wastes, including mechanical recycling such as shredding and milling,[5,6] pyrolysis at high temperature,[7,8] chemical decomposition using solvents such as methanol, ethanol, 1-propanol and acetone,[9–12] chemical recycling under sub-/supercritical conditions,[13–15] decomposition in high-temperature fluidized bed processes[16–18] and an electrochemical recycling method.[19] However, as shown in Table 1, the existing techniques generally suffer from various drawbacks such as requiring complicated processes and superior facilities, pollution generation and damage to the CFRP waste. Therefore, the remaining challenge is how to eliminate the epoxy resin without damaging the dimensions and properties of CFs in CFRPs through an environmentally friendly process. In order to overcome the challenge and fully utilize the high residual value of end-of-service-life CFRP composites, our research team has made great efforts in the past few years to investigate sustainable and affordable recycling technologies. In the present study, two new reaction conditions – KOH catalyst and temperatures – are considered to improve the recycling efficiency and the quality of rCFs. In addition, other key pro-

[a]*Guangdong Province Key Laboratory of Durability for Marine Civil Engineering, School of Civil Engineering, Shenzhen University, Shenzhen, Guangdong 518060, PR China. E-mail: xingf@szu.edu.cn*
[b]*School of Mechanical, Aerospace and Civil Engineering, University of Manchester, Manchester, M1 7JR, UK*

†Electronic supplementary information (ESI) available. See DOI: 10.1039/c8gc03672a

Table 1 Comparison between existing recycling methods and the new EHD method

Assessment		Methods					
		Mechanical[5,6]	Thermal			Chemical	EHD method
		Milling	Combustion[7,8]	Pyrolysis[7,8]	Fluidized bed[16–18]	Solvolysis[9–12]	Supercritical/subcritical[13–15]	
Facility	Temperature	Room temperature	1400–1600 °C	400–1000 °C	450–500 °C	~90 °C	400–650 °C	Room temperature
	Pressure	Atmospheric pressure	Atmospheric pressure	Atmospheric pressure	10–25 kPa	Atmospheric pressure	22.1–35 MPa	Atmospheric pressure
	Toxicity	Nontoxic	Nontoxic	Nontoxic	Nontoxic	Toxic	Toxic	Nontoxic
Performance	Waste size limit (length)	10–50 mm	NA	6–25 mm	5–10 mm	1 μm–50 mm	10–50 mm	No limit
	Residual tensile strength (*vs.* VCF)	50–65%	NA	50–85%	10–75%	85–98%	85–98%	89.46%
	Shear strength (*vs.* VCF)	Unreported	NA	NA	80%	Unreported	Unreported	120.74%
Environmental issues		Dust	Pollutant gas, dust, high energy use	Pollutant gas, high energy use	Pollutant gas, organic solvent, high energy use	Organic solvent	Organic solvent, high energy use	None

perties of the rCFs such as interfacial shear strength and surface roughness are thoroughly studied to have a better understanding of the feasibility for remanufacturing using rCFs. Furthermore, a more detailed microstructure analysis is carried out in the present study to analyse the degradation mechanism of the epoxy resin: the cyano group of the cross-linking agent dicyandiamide and the hydroxy group of the bisphenol-A type epoxy resin form amido bond during the curing process of the epoxy resin. Electrically driven heterogeneous catalytic reactions have been shown to enable the breaking of the C–N bonds of the amido bonds, thus leading to decomposition of the epoxy resin and reclamation of CFs with the benefit of the electrochemical promotion of catalysis (EPOC) effect.[20] Therefore, we reasoned that using a catalyst under these conditions should enhance this decomposition reaction, and we proposed the electrically driven heterocatalytic decomposition (EHD) method. In this study, CFRP composites were immersed in a NaCl electrolyte containing the KOH catalyst in the presence of electrical currents, and the effect of temperature was also investigated. With a view to optimize the reaction conditions to maximize the quality of the rCFs while minimizing the reaction time and energy input, we examined the effects of varying the applied current density, electrolyte concentration, catalyst concentration and temperature on the recycling of CFs. Mechanical tests and microstructural analyses are used to assess the mechanical properties and microstructures of the recycled fibres and to reveal the influences of the different reaction conditions. We found that the use of the catalyst and a moderately increased temperature with otherwise mild reaction conditions were key to obtaining high-performance CFs in an effective and efficient procedure. Finally, an optimized recycling method is suggested.

Our EHD method is the first green and cost-effective procedure for recycling high-strength CFs from commercial CFRP with no size limit (see Fig. 1). The chemicals used in this method are conventional, accessible and nontoxic. The easily implemented machinery and mild reaction conditions require low initial investments and energy consumption, which makes the economic value of the recycled fibres far higher than that of most existing recycled fibres. On top of the achieved merits, the research presented in this paper exploited the full potential of this new recycling technology and has a great potential for large-scale implementation.

Experimental section

Materials

The dimensions of the CFRP samples were 30 mm × 245 mm × 2 mm (width × length × thickness) (see Fig. SI1†). Each CFRP sample was divided length-wise into three regions: the test region (100 mm), which contained the rCFs; the protection region (80 mm), which insulated the test region; and the electrically conductive region (65 mm), which was connected to the power supply (see Fig. SI1†).

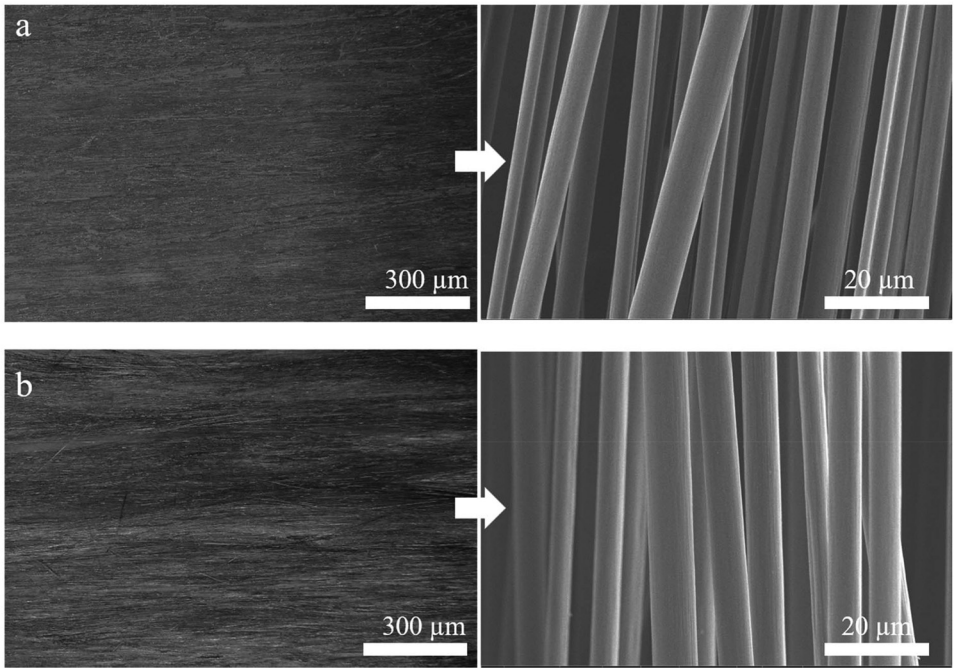

Fig. 1 Photographs of CFRP. (a) Virgin CFRP plate and (b) rCFs.

CFRP was purchased from Carbon Composites Company Limited (Hong Kong) with an epoxy resin content of 31.5%. Each layer of CF cloth is made by orthogonal weaving of longitudinal and transverse CFs. The CFs were T700-type produced by Toray Corporation, Japan, and the epoxy resin was LAM-125/226 type. The chemical composition of the epoxy resin provided by the manufacturer is shown in Table SI 2.†

Experimental setup

The recycling setup is shown in Fig. SI1(d).† The system was composed of four parts: (1) a DC power supply, providing unidirectional currents for the system; (2) the electrodes – CFRP served as the anode, which was connected to the positive electrode of the power supply, while a stainless-steel strip served as the cathode, which was connected to the negative electrode of the power supply; (3) an electrolyte solution (9L); and (4) a datalogger – HIOKI-LR8400 Datalog from HIOKI E.E. The datalogger monitored and measured the voltage of the sample, recording the data once per hour. The measured voltages can assess CF degradation and energy consumption in different recovery processes as explained in ESI.† In all tests, the CFRP sample (anode) was placed parallel to the stainless-steel strip (cathode). System voltage and energy consumption are shown in ESI (Fig. SI 2†).

Recycling process

The DC power supply was turned on to start the recycling process. The process was performed under laboratory conditions, and the solution volume was maintained throughout the experiment. At the end of the recycling process, the soft CFs were gently removed from the test sample with forceps and scissors. In order to reclaim 95% CFs from the composite wastes, the recycling process lasted for 72 hours at room temperature or 36 hours at elevated temperatures. The rCFs were then cleaned with alcohol by using an ultrasonic cleaner and rinsed three times (5 min each) with deionized water. The clean rCFs (Fig. 1) were placed in a dry box for three days at 50 °C.

Experimental parameters

In this study, three series of experiments were designed to investigate the effects of the reaction conditions – NaCl concentration, KOH concentration, current density, and temperature – on the rCFs. Detailed testing groups and experimental parameters are shown in Table SI 3.†

The first series of experiments investigated the effects of the current density and NaCl concentration. A total of 24 reaction conditions were considered, including six different current densities and four different NaCl concentrations. The six constant currents were 20, 40, 62.5, 78.1, 104.2, and 156.3 mA with the corresponding current densities of 3.33, 6.67, 10.42, 13.02, 17.37, and 26.01 A m^{-2}, respectively. The NaCl solution was prepared using deionized water and sodium chloride at concentrations of 0.5, 1.0, 2.0, and 3.0%. Note that when the currents were 78.1, 104.2, and 156.3 mA, no intact rCF could be obtained; therefore, characterization was not carried out for specimens subjected to these reaction conditions.

In the second series of experiments, which were based on the optimized conditions from the first series of experiments, the concentration of the catalyst (KOH) was varied. The selected currents were 20 and 40 mA, corresponding to the

current densities of 3.33 and 6.67 A m^{-2}, respectively, and the selected NaCl concentrations were 1, 2 and 3%. Three KOH concentrations were tested: 0.5, 1, and 1.5 g L^{-1}. Thus, a total of 18 reaction conditions were considered.

Similarly, in the third series of experiments, the optimized mix proportions obtained from the second series of experiments were used, that is, two currents (20 and 40 mA), one NaCl concentration (2%) and one KOH concentration (1 g L^{-1}). In addition, the recycling reactions were carried out at 40, 60 and 75 °C. Thus, a total of six reaction conditions were tested.

Characterization

Thermogravimetric analysis. Thermogravimetric analysis was used to determine the residual mass of the epoxy resin in the rCFs. An STA409PC model thermal analyser made by the NETZSCH Group in Germany was used. The temperature was increased by 10 °C min^{-1} to an upper limit of 800 °C, and the nitrogen flow rate was 100 cm^3 min^{-1}. Three analyses were performed under each reaction condition, and the average results are reported (see Table SI1†).

Tensile tests on CFs. To evaluate the residual tensile strength of the rCFs, tensile tests on CF monofilaments were conducted according to the standard ISO 1156620.[21] A Nano UTM 150 Nano-stretcher (American Agilent Technologies Inc.) was used with the test system UTM-Bionix Standard Toecomp Quasistatic. The test parameters were set as follows: loading of 750 μN, tensile rate of 0.2 μm s^{-1}, loading resolution of 50 nN, displacement resolution of <0.1 nm, tensile resolution of 35 nm, and maximum displacement of the actuator of ±1 mm. The temperature was 20–30 °C, and the ambient relative humidity was 40% during the test. A total of 20 replicate tests have been conducted for each reaction condition (see Table SI4†).

Diameter measurements on CF monofilaments. The diameter of the CF monofilaments was measured by using a 250A Helium–Neon laser gauge from Changchun New Industrial Optoelectronics Technology Co., Ltd. The CF monofilament was placed on the sample holder, and its diffractive dark-fringe spacing was measured. The precise diameter of the monofilament was then calculated according to the diffraction principle. A total of 20 replicate tests have been conducted for each reaction condition (see Table SI5†).

Interfacial shear strength (IFSS) tests on CF monofilaments. The IFSS between the CFs and the epoxy resin could be measured by using the microdroplet test.[22] The CF monofilament was straight fixed on the positioning hole of the concave type paper. Paste glue was used to fix both ends of the fibre and was air dried naturally for one day. Upon gelatinization, the sample is placed in the foam-plate slot and solidified naturally for 24 h. The HM410 composite material interface evaluation device was manufactured by Japan Toei Co. Ltd. The test parameters were a loading speed of 0.12 mm min^{-1} and a microscope magnification of 2 times. Before testing, the diameter of the resin droplet was measured by using a high-magnification microscope. Five monofilaments from each reaction condition were tested, and the mean averages of the results were used for the assessment (see Table SI6†).

Environmental scanning electron microscopy tests. To observe the surface characteristics of the rCFs, samples were imaged by using an environmental scanning electron microscopy (Quanta TM 250 FEG model) from FEI Company, USA. The scanning was conducted in a high-vacuum environment; the working distance was approximately 10 mm; and the test acceleration voltage was 20 kV. The sample was coated with a layer of gold before testing.

Atomic force microscopy tests. The ICON-PT-PKG scanning probe microscope produced by Brooke Inc., USA, was used to scan the micromorphology of the rCF surface; both 2D and 3D images were obtained. In this study, the scanning area was 4 μm × 4 μm, and the scanning rate was set to 1.0 Hz. An illustration of the test setup can be found in ref. 32. Before testing, the glass slide was cleaned using alcohol on cotton, and then, a double-sided adhesive was glued onto the glass slide before carefully sticking the CF onto the adhesive. The CF was ≥20 mm. The obtained images were analysed by using NanoScope Analysis 1.8 with R_a values to represent the surface roughness. A total of 20 replicate tests have been conducted for each reaction condition (see Table SI 7†).

X-ray photoelectron spectroscopy. A photoelectron spectrometer (ULVAC-PHI VPII model) was used to determine the elements and functional groups on the CF surfaces. With the help of the XPS Peak 4.1 software, the functional group content was derived by curve fitting based on Gaussian and Lorentzian functions. The X-ray source of the monochromator was the aluminium target. A full-spectrum scan on the rCFs was first conducted, followed by narrow-band and high-resolution scans of C 1s at an incident angle of 90°. The elements measured were C, Si, N, O, and Cl. A total of 10 replicate tests have been conducted for each reaction condition.

Results and discussion

Degradation of epoxy resin

The key factors in recycling CFs from CFRP waste are the degradation of the epoxy resin and the extent of its removal, which was measured in this study by thermogravimetric analysis. A greater extent of epoxy resin removal results in cleaner reclaimed fibres. Table 2 shows that with increasing NaCl concentration, the extent of epoxy resin removal first increased and then decreased; the experiments performed with 2% sodium chloride (NaCl) provided the greatest extent of epoxy resin removal. At 40, 60 and 75 °C, CFs were obtained after 36 hours with 99.3%–99.9% of the epoxy resin removed (see Table SI 1†). The results show that increasing the reaction temperature can significantly increase the epoxy resin decomposition efficiency. To reclaim 95% CFs from the composite wastes, the reaction time needed for the high temperature condition is only half of that at room temperature.

Note that the maximum reaction temperature in this study was 75 °C, which is far lower than the temperature required

Table 2 The mechanical properties of the rCFs

Test unit	Specimens	Extent of epoxy resin removal (%)	Tensile strength (GPa)	Residual strength (%)	Diameter (μm)	IFSS (MPa)	Residual strength (%)	Failure modes	R_a (nm)
	VCF	—	4.641	100.00	7.00	31.00	100	DB	201
1	I20S0.5	68.3	2.634	56.76	6.97	—	—	—	—
	I20S1	89.6	3.472	74.81	6.95	—	—	—	—
	I20S2	95.8	3.768	81.19	6.96	—	—	—	—
	I20S3	90.4	3.488	75.16	6.96	—	—	—	—
	I40S0.5	67.1	2.583	55.66	6.96	—	—	—	—
	I40S1	89.3	3.417	73.63	6.95	—	—	—	—
	I40S2	93.7	3.693	79.57	6.95	—	—	—	—
	I40S3	89.8	3.458	74.51	6.95	—	—	—	—
	I62.5S0.5	63.3	2.386	51.41	7.12	—	—	—	—
	I62.5S1	65.5	2.471	53.24	6.97	—	—	—	—
	I62.5S2	68.5	2.562	55.20	6.92	—	—	—	—
	I62.5S3	66.1	2.509	54.06	6.94	—	—	—	—
2	I20S1K0.5	99.7	3.399	73.24	6.93	29.69	95.77	CB	195
	I20S1K1	99.6	3.165	68.20	6.91	33.48	108.00	DB	214
	I20S1K1.5	100.0	2.952	63.61	6.85	32.76	105.68	DB	205
	I20S2K0.5	99.8	3.426	73.82	6.94	29.50	95.16	CB	196
	I20S2K1	99.7	3.310	71.32	6.90	37.43	120.74	DB	219
	I20S2K1.5	99.5	3.021	65.09	6.87	33.06	106.65	DB	213
	I20S3K0.5	99.9	3.413	73.54	6.93	28.83	93.00	CB	193
	I20S3K1	99.7	3.198	68.91	6.92	34.06	109.87	DB	209
	I20S3K1.5	99.6	2.966	63.91	6.86	33.65	108.55	DB	203
	I40S1K0.5	99.7	3.357	72.33	6.87	—	—	—	—
2	I40S1K1	99.6	2.980	64.21	6.85	—	—	—	—
	I40S1K1.5	99.6	2.666	57.44	6.81	—	—	—	—
	I40S2K0.5	99.4	3.365	72.51	6.88	27.00	87.11	CB	185
	I40S2K1	99.8	2.776	59.81	6.84	28.08	90.57	DB	199
	I40S2K1.5	99.6	2.735	58.93	6.82	24.70	79.69	CB	175
	I40S3K0.5	99.5	3.348	72.14	6.87	26.53	85.58	CB	189
	I40S3K1	99.8	2.910	62.70	6.85	28.33	91.39	DB	197
	I40S3K1.5	99.3	2.660	57.32	6.82	25.20	81.29	CB	178
3	I20S2K1T40	99.5	3.759	81.00	6.99	25.42	82.00	CB	190
	I20S2K1T60	99.9	4.045	87.16	7.00	33.59	108.35	DB	203
	I20S2K1T75	99.8	4.083	87.98	6.99	33.72	108.77	DB	208
	I40S2K1T40	99.3	3.758	80.76	7.00	24.61	79.39	CB	195
	I40S2K1T60	99.4	4.126	88.90	6.98	29.84	96.26	DB	199
	I40S2K1T75	99.7	4.152	89.46	6.99	35.79	115.45	DB	211

I = current; I20 = 20 mA; S = salt; K = KOH; K0.5 = 0.5 g L^{-1} KOH; T = temperature; T40 = 40 °C; DB = debonding failure within the epoxy resin; CB = debonding failure at the interface of the CFs and the epoxy resin.

for thermal decomposition of the epoxy resin (*i.e.*, in the range of approximately 300 to 600 °C under nitrogen or air atmosphere). Therefore, the enhanced extent of epoxy resin removal is not due to thermal decomposition of the epoxy resin. Rather, it is related to the mutual synergy between the high temperature and the catalyst (KOH). Further increasing the temperature will likely lead to a continuous increase in the extent of epoxy resin removal. However, higher temperatures might increase the requirement of the machinery, resulting in a greater initial investment. Therefore, the upper limit of temperature considered in this study is 75 °C.

The diameters of the rCFs are presented in Table 2. The results show that the diameter of the rCFs only slightly decreased compared to that of the new fibres prior to incorporation into a composite material VCF with a diameter of 7 μm, which shows intact CFs without damage to dimensions could be reclaimed from the proposed recycling technology. Under the same current density, when the catalyst (KOH) concentration was 1.5 g L^{-1}, the diameter of the rCF was the smallest. The diameters of the rCF obtained at high temperatures (40, 60 and 75 °C) were generally the same.

Mechanical properties of rCF

Residual tensile strengths of rCF. Table 2 and Fig. 2 show the residual tensile strength of rCF monofilaments under different reaction conditions. Compared to that of the VCF (tensile strength of 4641 MPa), the residual tensile strength of the rCFs from the optimized conditions slightly decreased.

The tensile strengths of the rCF decreased with the increasing current density – a slight decrease from 20 mA to 40 mA and a profound decrease from 40 mA to 62.5 mA (see Table 2). The long-term action of a high current density may damage

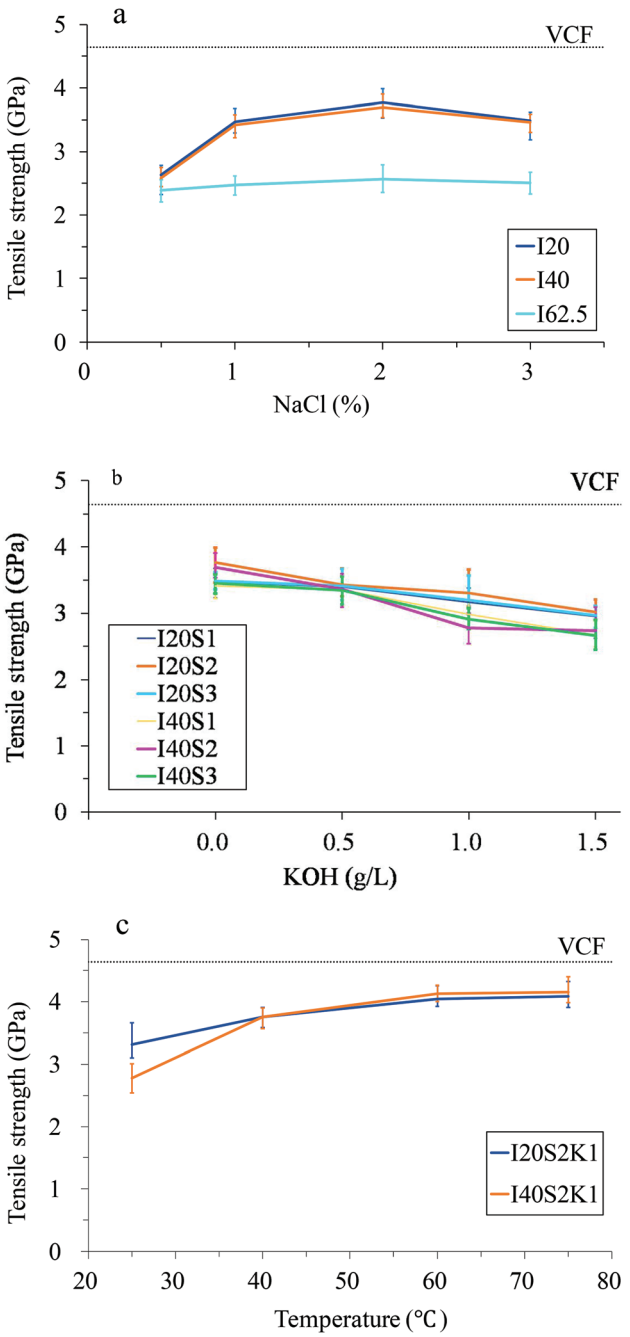

Fig. 2 The tensile strength values of the rCFs. For an explanation of the sample numbers, see Table 2. (a) Effect of NaCl concentration; (b) effect of KOH concentration; (c) effect of temperature.

the bulk structure of the CFs. When the current densities were 3.33 A m^{-2} and 6.67 A m^{-2} (I20 and I40 series), the tensile strengths of the rCF were much better than those of the other series (Fig. 2a). As shown in Fig. 2a, as the NaCl concentration increased from 0.5% through to 3%, the tensile strengths of the rCF first increased, reaching a maximum residual tensile strength of 81.19% at 2.0% NaCl (with a current of 20 mA) and then decreased. Fig. 2b shows that the residual tensile strength of the rCF does not improve with an increase in the KOH concentration. It is indicated that the high KOH concentration might exacerbate the oxidation of CFs and cause them mechanical damage. Conversely, KOH can significantly improve the extent of epoxy resin removal and increase the interfacial shear strength, which is discussed below. The results show that the residual tensile strength of the rCF increased with temperature (Fig. 2c). The increase was most significant from 25 to 40 °C and less significant in the range of 40 to 60 °C, whereas there was almost no change from 60 to 75 °C. The residual tensile strengths of the rCF treated at 75 °C with currents of 20 and 40 mA (specimens I20S2K1T75 and I40S2K1T75) reached 4.083 GPa and 4.152 GPa, respectively, which were 87.85% and 89.83% relative to VCF strength.

The matrix of the CF in the mechanical process of recycling has suffered severe damage, and long clean recycled fibres cannot be obtained. The residual strength of the rCF is 50 to 65% of that of VCFs.[5,6] Although the mechanical process can result in cleaner, shorter lengths of CFs through thermal decomposition, due to the high temperature and surface oxidation, the mechanical properties of the CF are reduced to 50%–85%.[7,8] Taking advantage of the dissolvability of super-/subcritical fluid to the polymer materials, clean CF can be obtained with the maximum retention (85%–98%) of the original mechanical properties of the CF *via* the solvolysis method.[11–14] However, the demanding reaction conditions increase the requirements on the facilities and restrain the size of the rCF. The residual strength of the rCF obtained using the EHD method is far higher than that obtained using mechanical recycling and thermal decomposition, but slightly lower than that obtained by solvolysis.

Shear strengths of the rCF. The interfacial shear strength (IFSS) between the rCF and epoxy resin is also one of the key mechanical properties, which was measured by the microdroplet test. The test has two failure modes: debonding failure within the epoxy resin (DB) and debonding failure at the interface of the CFs and the epoxy resin (CB). The measured IFSS of the VCFs was 31 MPa with the DB failure mode. At the point of failure, the CFs and epoxy resin are still strongly bonded without cracks on the surface, and the epoxy resin becomes the weak part. The IFSS is only measured for the rCF of I20 and I40 series due to the unfavourable properties of the rCF reclaimed from other current density conditions. Results are presented in Table 2 and Fig. 3, and the failure modes are shown in Fig. 4.

Higher current densities led to lower IFSS values of the rCF. When the NaCl concentration was increased from 1 to 3%, the IFSS of the rCF first increased, reaching a maximum value at 2% NaCl, and then decreased again. The IFSS of all samples of the rCF increased when the KOH concentration increased from 0.5 to 1.0 g L^{-1} but declined as the KOH concentration continued to increase from 1.0 to 1.5 g L^{-1} (Fig. 3a). In the I20 series, the lowest IFSS of the rCF was obtained when the KOH concentration was 0.5 g L^{-1}, which was 4.23 to 7.0% lower than that of the VCFs. However, at KOH concentrations of 1.0 and 1.5 g L^{-1}, the IFSS values for the rCF were higher than that of the VCFs. The IFSS of the rCF from specimen I20S2K1 was the

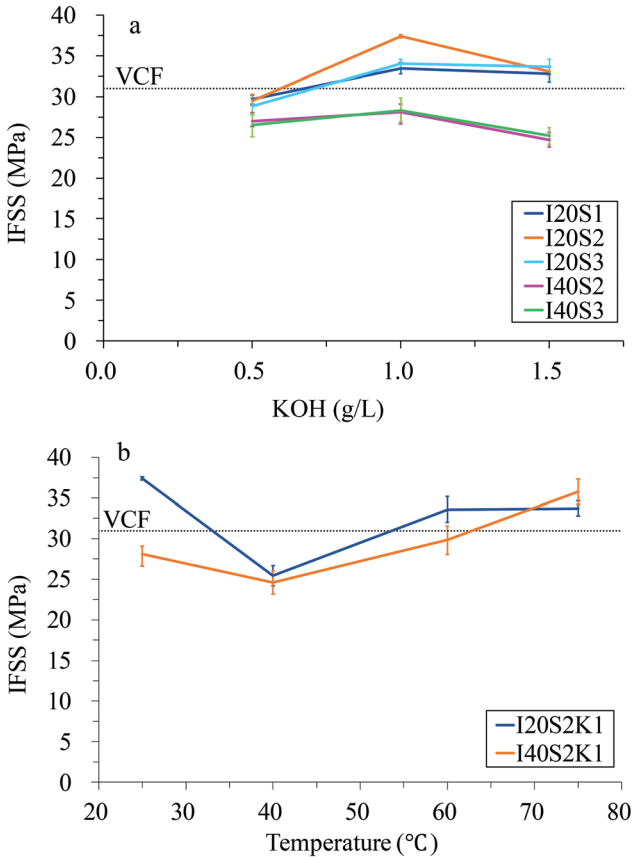

Fig. 3 Shear strengths of the rCFs. For an explanation of the sample numbers, see Table 2. (a) Effect of KOH concentration; (b) effect of temperature.

highest (37.43 MPa), which was 20.74% higher than that of the VCFs. In the I40 series, on the other hand, the IFSS values for all rCF were lower than that of the VCFs. When the KOH concentration was ≥1.0 g L^{-1}, the DB failure mode occurred. The relationship between the IFSS of the rCF and temperature is presented in Fig. 3b. When the temperature increased from 25 to 40 °C, the IFSS of the recycled I20 and I40 CFs dropped from 37.43 and 28.08 MPa to 25.42 and 24.61 MPa, respectively. For both samples of CF recycled at 40 °C, the failure mode was CB, the epoxy resin and CFs completely debonding, leaving barely a trace of the epoxy resin residue on the CF surface. As the temperature was increased to 60 °C, the IFSS also increased. The IFSS values of the recycled I20 and I40 CFs were 33.59 and 29.84 MPa, respectively, which are 108.35 and 96.26% of that of the VCFs. The failure mode was DB for both samples. When the temperature reached 75 °C, the IFSS values of the recycled I20 and I40 CFs were 33.72 and 35.79 MPa, respectively, which are 108.77 and 115.45% of that of the VCF; similarly, the failure mode was DB. The surface of the epoxy resin at the point of failure displayed prisms and asperities, which increased the area of the failure surface. In particular, the rCF from the I40 condition exhibited vigorous debonding and internal fracture of the droplets due to the strong force at failure. The above results show that decreasing the recycling period will reduce oxidative etching on rCF, whereas increasing the temperature will increase the surface roughness and impregnation.

Microstructural characterization of rCF

Surface morphology. The morphology of CF surfaces can be visualized by scanning electron microscopy (SEM). Since the surface morphology can reveal the degree of damage suffered in the recycling process and this can be related to the observed residual tensile strength of the rCF, we used SEM to analyse the surfaces of the rCF.

The SEM images of the rCF from the I20 and I40 series with the presence of KOH (where the current was set to 20 and 40 mA, respectively) show that all the resin was completely removed (Fig. 5), indicating that KOH can effectively decompose the epoxy resin. Very few defects were observed on the surface of the rCF obtained at a low current density and at both low and high NaCl concentrations. In the presence of high current densities or low NaCl concentrations, more oxygen is generated on the CFRP surface, and CFs are strongly oxidized and etched. In these cases, the SEM images (Fig. 5g and h) show that the surface layer of the rCF is degraded, and the decreased residual tensile strength can be attributed to the defects.

The concentration of KOH catalyst is very important in this EHD process. Cl_2 was generated at the anode region during electrolysis in the presence of Cl^- (eqn (1)). Part of the gas reacted with water to form more oxidizing HClO (eqn (2)). ClO^- would oxidize the epoxy resin by breaking down the C–N bond.[19,23,24] It is critical to adjust the concentration of the KOH

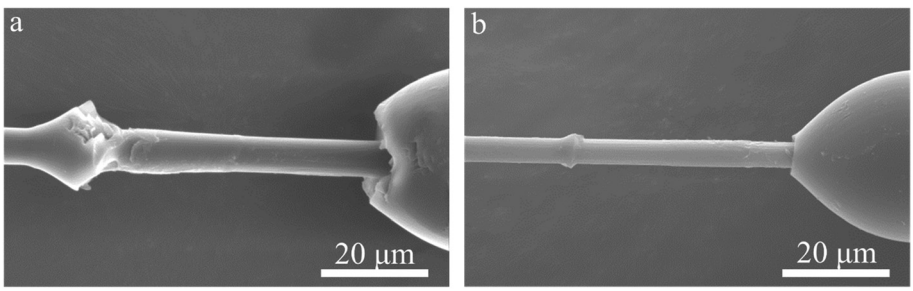

Fig. 4 Interface failure modes between the rCF and epoxy resin. (a) DB mode; (b) CB mode.

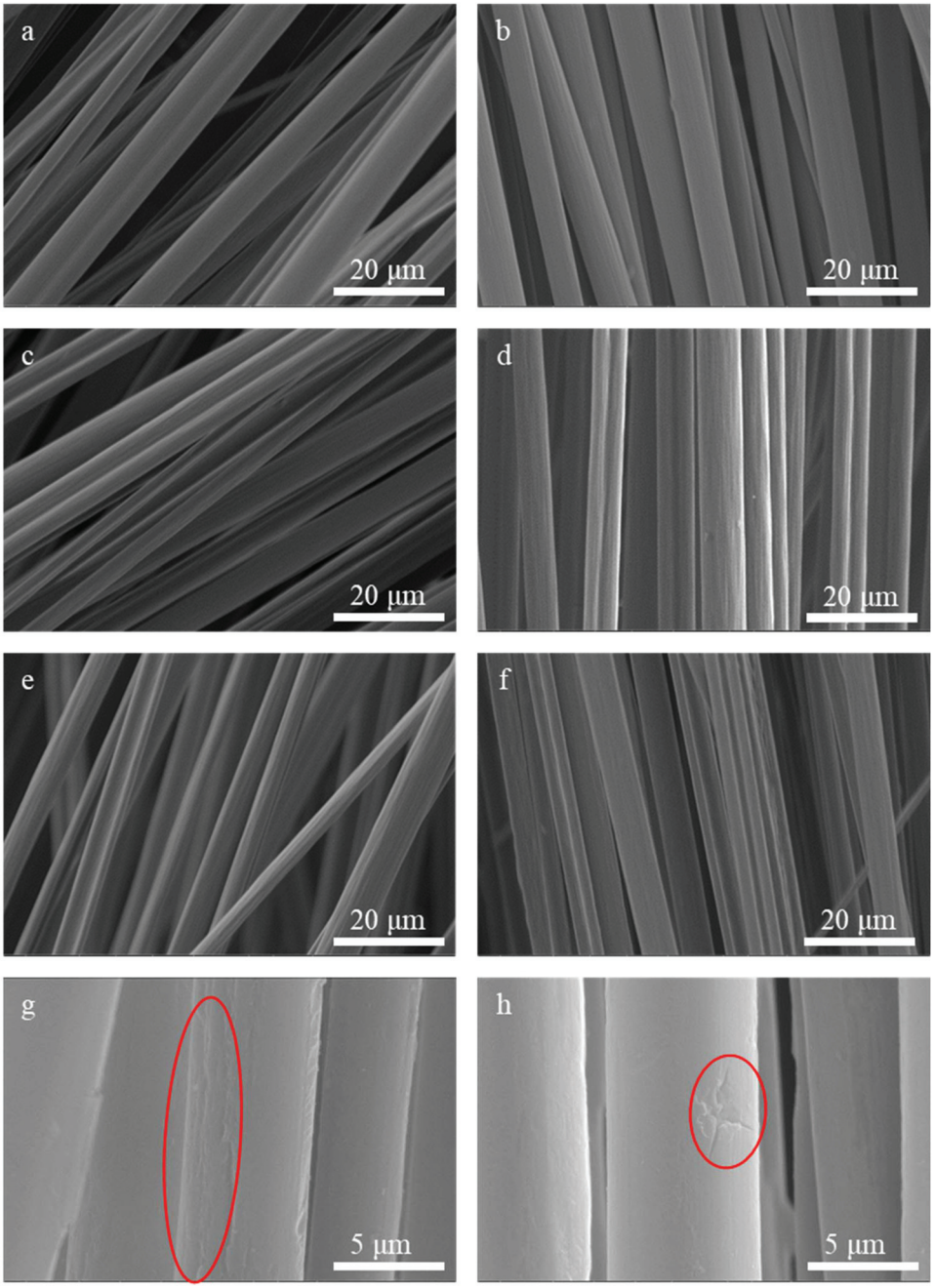

Fig. 5 SEM images of the I20 and I40 series. For an explanation of the sample numbers, see Table 2. (a) Specimen I20S2K0.5; (b) specimen I40S2K0.5; (c) specimen I20S2K1; (d) specimen I40S2K1; (e) specimen I20S2K1.5; (f) specimen I40S2K1.5; (g) etchings and longitudinal grooves on specimen I20S2K1; (h) etchings and longitudinal grooves on specimen I20S2K1.5.

catalyst in order to optimize the performance of the recycling method because of the following two reasons. First, when KOH was added as a catalyst, H^+ would react with OH^- to form H_2O, pushing the second reaction to the right side. Therefore, more ClO^- would be formed, leading to the increased degradation efficiency of the epoxy resin. Due to the ionic intercalation in the electrochemical process, OH^- ions would be inserted into the fibre surface and graphite layer, leading to carbon fibre cortex inflation. This phenomenon also increased the degradation of the epoxy resin and the recovery of the carbon fibres. Second, in the presence of excess OH^-, the OH^- would attach to the carbon atom surface. The adjacent carbon atoms and the adhered OH^- would react to form oxygen, resulting in the oxidation etching effect on the carbon fibre surface. The reaction process is given in eqn (3) and (4):.

$$2Cl^- \rightarrow Cl_2 + 2e^- \quad (1)$$

$$Cl_2 + H_2O \rightarrow HClO + H^+ + Cl^- \quad (2)$$

$$C_s + OH^- \rightarrow C_sOH_{adsorb} + e^- \quad (3)$$

$$4C_sOH_{adsorb} \rightarrow 2H_2O + O_2 + 4C_s \quad (4)$$

When the KOH concentration is 0.5 g L^{-1} (Fig. 5a and b), the surface of the CFs is relatively smooth and the curvature is unchanged, and there are no visible longitudinal grooves. This indicates that the CFs are not damaged, which explains why the tensile strength of these CFs was only slightly lower than those obtained using reaction conditions without KOH. With an increase in the KOH concentration, the oxidation-induced etching on the CFs and intercalation of OH^- ions become pronounced. Therefore, longitudinal grooves can be observed on the CF surface, as shown in Fig. 5c–f. This degradation was more severe in the I40 series. Cracks can even be seen on the CF surfaces of specimens I40S2K1 (59.81% of that of the VCF) and I40S2K1.5 (58.93% of that of the VCF). For more detailed observations, these two specimens were scanned at a higher magnification of 20 000. Fig. 5g shows a small etched part of the rCFs with a reduced cross-sectional area and clear longitudinal groove structures. In Fig. 5h, the surface of the CFs has deteriorated due to oxidation and exhibits pits and crack defects.[10,13,14] When the tensile test is conducted on a single fibre, this part becomes the critical section, and the stress concentration occurs near this section. Finally, fracture failure occurs in this section.

Similarly, at elevated temperatures, the rCFs were generally found to be clean. At 40 °C, although several tiny epoxy particles could be seen on the CF surface, the CFs were otherwise clean, with no physical defects such as cracks or pits. When the temperature was increased to 60 and 75 °C, the epoxy resin was not visible at all on the CF surface; similarly, there were no visible physical defects, and furthermore, the CFs from specimen I40S2K1T75 had the highest residual tensile strength.

Note that CFs can be recycled within 36 hours at high temperature, which is only half of the time required at ambient temperature. Thus, at high temperature, CFs are exposed to the electrolyte for a shorter duration, which means that damage to the rCF due to electrochemical oxidation etching, OH^- ion intercalation reactions and alkali corrosion will be less than at ambient temperature. This is the reason for the higher residual tensile strength of the CFs recycled at elevated temperatures.

Surface roughness. We analysed the surface structure of the rCFs by atomic force microscopy (AFM), from which the surface roughness value, R_a, can be obtained. The surface roughness of rCFs is an important factor influencing mechanical interlocking and impregnation. AFM images show that when the KOH concentration was 0.5 g L^{-1}, the degradation of the epoxy resin was mild and the CF surface was smooth (see Fig. 6c and d). The calculated roughness (R_a = 195 nm) was slightly lower than that of the VCFs (R_a = 201 nm), causing a slight decrease in the IFSS of the CFs. When the KOH concentration was increased to 1.0 g L^{-1}, the degradation of the epoxy resin was accelerated, and the relatively severe electrochemical oxidation caused a narrow longitudinal groove structure and a high roughness value (R_a = 219 nm) (see Fig. 6e and f). These trenches with a small width not only increase the mechanical interlocking between the CFs and epoxy resin, but also significantly increase the specific surface area and improve the epoxy resin impregnation. As the KOH concentration was further increased to 1.5 g L^{-1}, the intercalation of OH^- ions increased, and the corresponding R_a value was calculated as 213 nm (see Fig. 6g and h). Therefore, the strength was higher than that of the VCFs. The R_a values increased, and the adhesiveness also increased, leading to an increase in the IFSS because more intercalation reactions occur at higher temperatures, resulting in a larger specific surface area, increased roughness and a better impregnation of CFs. The mechanical interlocking effect at the interface was enhanced, which creates an anchoring effect and increases the IFSS.

Surface chemical composition. X-ray photoelectron spectroscopy (XPS) was used to determine the elements and functional groups on the CF surfaces. We scanned the full spectrum (Fig. 7a, c, e and g) and C 1s spectrum (Fig. 7b, d, f and h) of VCF and rCFs. After peak fitting, five peaks could be identified: two main peaks, C (284.6 eV) and O (532.0 eV), and three minor peaks, Si (99.5 eV), Cl (199.8 eV), and N (399.5 eV). The detailed element contents are shown in Table 3. The surface carbon and oxygen contents of the VCFs were 75.2 and 18.3%, respectively, and the O/C ratio was 0.2434. The surface oxygen content of the CFs increased through the electrochemical recycling process. The increased oxygen content implies an enhancement in the surface defects and surface activities of the CFs, thereby decreasing the tensile strength and increasing the IFSS. The experimental results show a proportional relationship between the O/C ratio of the CFs and the IFSS, which is consistent with the results reported by Jin *et al.*[25] and Zhu *et al.*[26] Minimal oxidation of CFs occurs at a NaCl concentration of 2.0%, leading to the highest residual tensile strength among all the reaction conditions tested. The oxygen content increased by more than 20% compared with that of the VCFs with an increase in the KOH concentration. In the presence of KOH, oxidative etching on CF surfaces is exacerbated, which decreases the tensile strength but increases the IFSS. At elevated temperatures, the rCFs had a slightly lower content of carbon on their surface than the VCFs according to XPS results. Oxidation might have caused a small number of carbon particles to be removed from the CF surface. However, the oxygen content and ratio of oxygen to carbon increased, which indicates that the CFs underwent oxidation during recycling and their surface activity increased.[27]

The C 1s high-resolution narrow spectrum can be divided into six chemical bond regions by peak-fitting: graphene C–C (284.4 eV), amorphous C–C (284.8 eV), C=O (285.5 eV), C–O (286.2 eV), C–Cl (287.2) and O–C=O (288.5 eV).[22–26] The VCFs have relatively few oxygen-containing functional groups on their surface (the total content of C–C bonds in graphite and

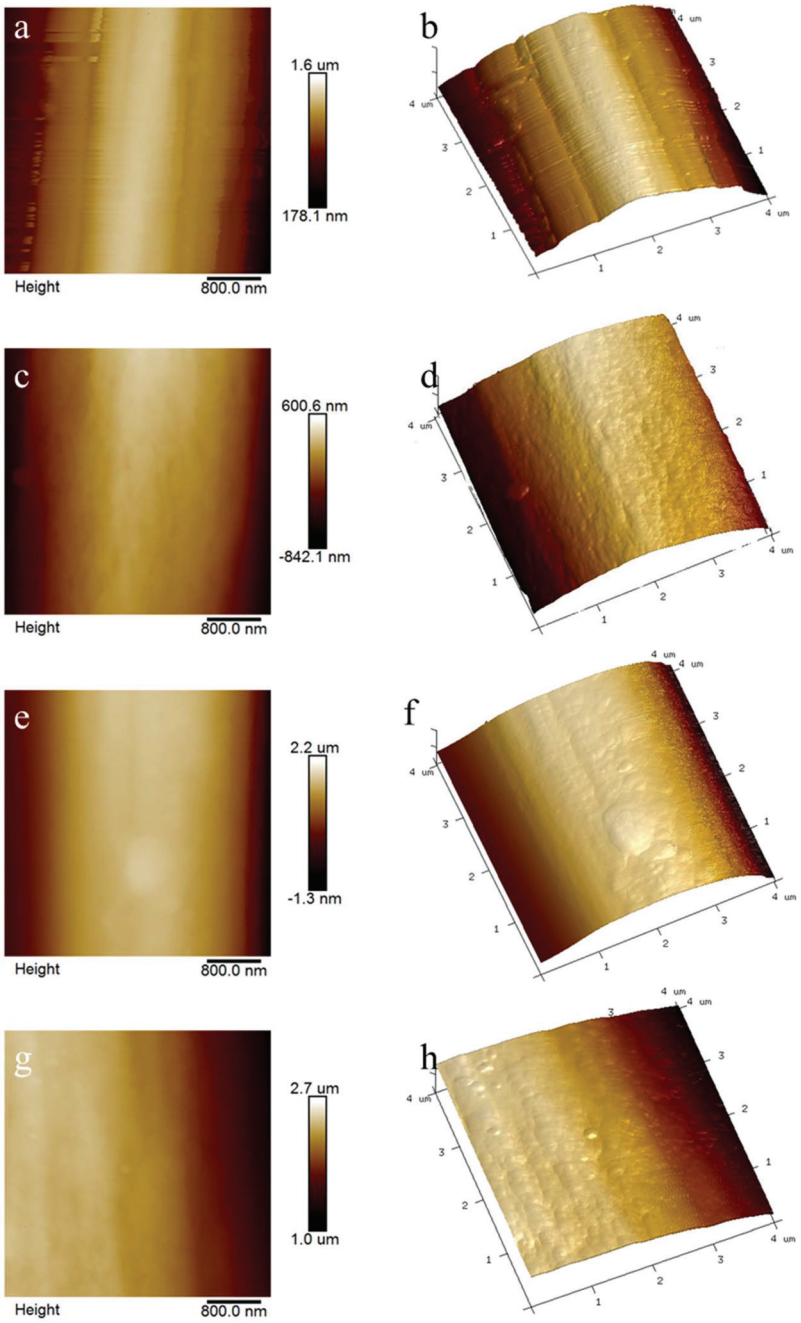

Fig. 6 AFM images of VCF and rCFs. For an explanation of the sample numbers, see Table 2. (a) 2D image of VCF; (b) 3D image of VCF; (c) 2D image of I20S2K0.5; (d) 3D image of I20S2K0.5; (e) 2D image of I20S2K1; (f) 3D image of I20S2K1; (g) 2D image of I20S2K1.5; (h) 3D image of I20S2K1.5.

amorphous states is 69.3%, whereas the content of various C–O bonds is 30.7%). Consequently, they are relatively surface-inactive and water repellent. More C–O functional groups would increase their hydrophilicity and their propensity to impregnate polymer matrices such as epoxy resins.[28] In addition, oxygen-containing reactive functional groups such as –COOR can increase the reaction between the CFs and epoxy resin, generating strong covalent bonds and improving interfacial bonding.[29,30] A larger number of oxygen-containing functional groups might be expected to increase the chemical interactions between the CFs and epoxy resin, which might be the reason for the increased interfacial shear stress, which is consistent with the findings of other studies.[31,32] Increasing the concentration of NaCl in the electrolyte solution (from 1.0% to 2.0%, *i.e.* specimen I20S1K1 and I20S2K1) led to an increase in the number of C–C bonds, as observed by the XPS scan, but the number of bonds decreases if the concentration of NaCl is decreased from 2 to 3.0% (*i.e.* specimen I20S2K1

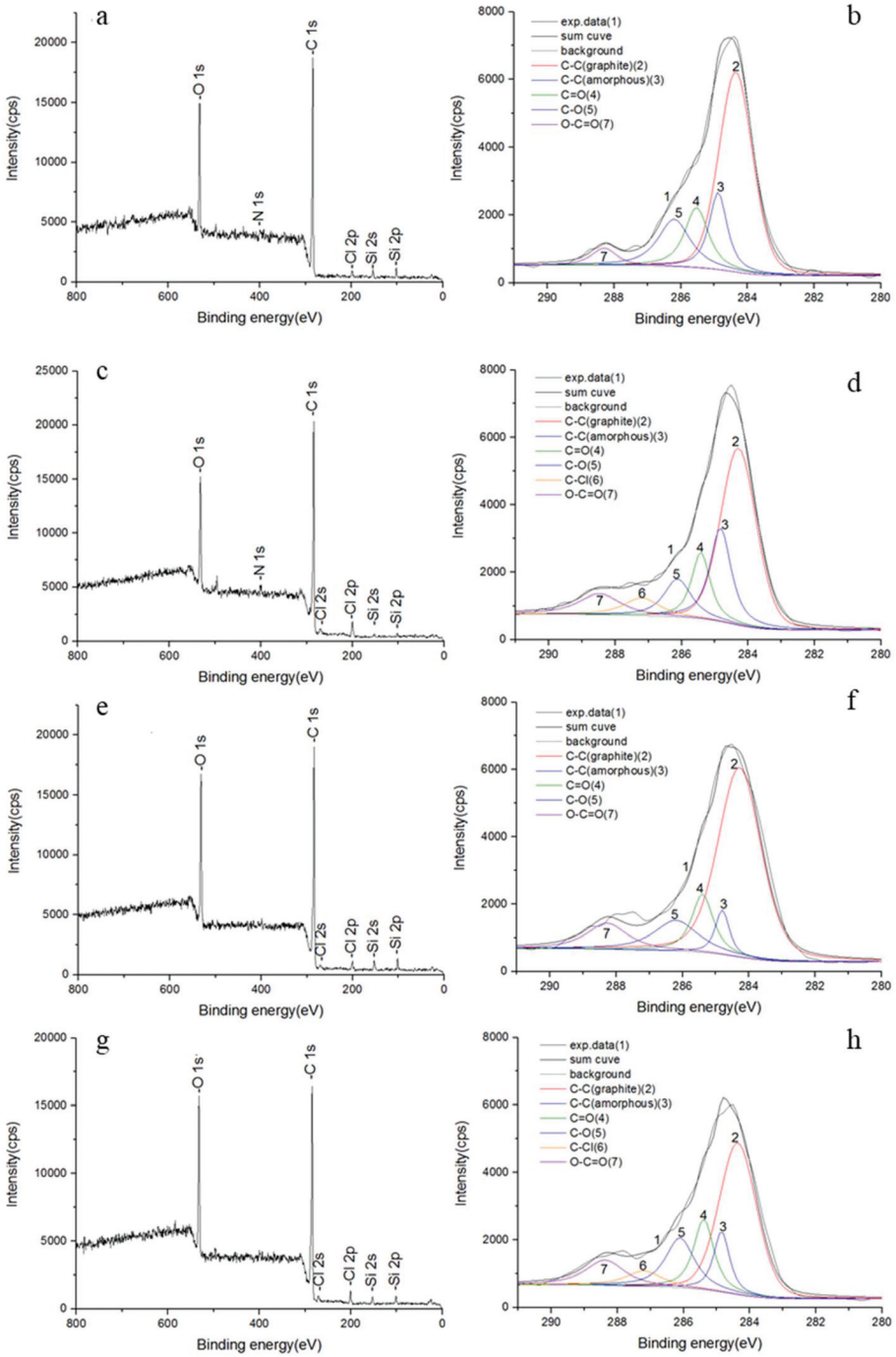

Fig. 7 XPS spectra of VCF and rCFs. For an explanation of the sample numbers, see Table 2. (a) Full spectrum of VCF; (b) C 1s spectrum of VCF; (c) full spectrum of I20S2K0.5; (d) C 1s spectrum of I20S2K0.5; (e) full spectrum of I20S2K1; (f) C 1s spectrum of I20S2K1; (g) full spectrum of I20S2K1.5; (h) C 1s spectrum of I20S2K1.5.

and I20S3K1). Additionally, the O/C ratios of CFs recycled at higher temperatures (36 hours) were lower than those obtained at room temperature (72 hours) due to a shorter oxidation period. The fitting results show that the C–Cl bond content of both the higher-temperature rCF and VCF was 0, which indicates that those rCFs are not substantially corroded by chlorine. Compared to the VCFs, the total content of graphene and amorphous C–C bonds on the surface of the rCF decreased. Additionally, both the C═O bond and C–O bond contents increased slightly; the O–C═O bond content was two to three times more than that of the VCFs.

Thus, the surface chemical components are an important factor influencing the mechanical properties of rCFs. The CFs recycled from specimens I40S2K1T75 and I20S2K1 had

Table 3 Element and functional group content of the surfaces of VCFs and recycled carbon fibres (%)

Specimen no.	C	O	Cl	N	Si	O/C	C–C (graphene)	C–C (amorphous)	C═O	C–O	C–Cl	O–C═O
VCF	75.2	18.3	0.9	3.1	2.5	0.2434	54.9	14.4	14.6	15.5	0.0	4.0
I20S2K0.5	74.2	19.7	2.2	3.1	0.8	0.2655	48.4	19.3	12.0	10.1	6.3	8.4
I20S2K1	73.1	23.3	1.3	0.0	1.3	0.3187	64.8	5.9	12.0	12.9	0.0	10.1
I20S2K1.5	73.0	23.3	1.5	0.0	2.2	0.3192	47.6	10.3	15.1	15.4	6.0	10.3
I20S1K1	74.8	20.8	1.9	2.3	0.2	0.2781	49.7	11.1	18.2	12.5	0.0	13.4
I20S3K1	72.7	20.4	4.3	0.8	1.8	0.2806	56.2	6.6	15.4	15.3	1.9	9.7
I40S2K1	72.6	20.8	3.7	2.9	0.0	0.2865	36.9	16.4	19.0	15.6	6.8	10.1
I20S2 K1T40	74.3	22.0	1.6	0.9	1.2	0.2961	35.6	20.9	18.0	18.1	0.0	12.0
I20S2 K1T60	74.4	21.5	1.1	0.6	2.4	0.2890	49.7	11.8	17.2	15.0	0.0	11.1
I20S2 K1T75	72.8	21.1	3.7	0.9	1.5	0.2898	52.8	10.1	14.6	16.7	0.0	10.7

the greatest residual tensile strength and highest IFSS, respectively.

Discussion

During the recycling process, the C–N bonds of the amido bonds ruptured, followed by the cleavage of ether, benzyl and secondary and tertiary amine groups. Afterwards, the epoxy matrix on the CFRP surface was degraded gradually and subsequently the CFs were exposed to the electrolyte. Electrochemical oxidation and etching cause damage to the CFs. The rCFs suffer oxidation and OH^- ion intercalation, resulting in swelling of the outermost layer and increasing the surface roughness, and thus lower residual tensile strengths but higher interfacial shear strengths.

Conclusions

In this study, we investigated the recycling of a CFRP composite by using an aqueous electrolyte solution in the presence of electrical currents. The C–N bonds of the epoxy resin can be broken in an electrically driven heterogeneous catalytic reaction, leading to the decomposition of the resin component and recovery of CFs *via* the benefit of the EPOC effect. The properties of the rCFs are depended on the combined effect of all the variables. By optimizing the working conditions, depolymerization of the epoxy resin and reclamation of the CFs are found to be efficient even under ambient temperature and pressure using conventional and nontoxic chemicals. This method achieves a high (nearly 100%) extent of epoxy resin removal. The average residual tensile strength and IFSS are approximately 90% and 120%, respectively, of those of VCFs. Compared with existing recycling methods, this new method is simple and green (see Table 1). The commercial value of the recycled fibres based on the proposed technology is expected to dramatically increase, since (1) the simplicity of the procedure and low facility demand will remove the size restraint on the composite waste and (2) the dimensions and strength of CFs can be maintained in the recycling procedure. In addition, this technology can be implemented in an overall cost-effective manner on a large scale and will profoundly impact the management of CFRP composites and possibly other thermoset waste materials. This study is part of a realistic development process towards the longer-term goal of industrial-scale CFRP processing.

Conflicts of interest

There are no conflicts to declare.

Acknowledgements

The authors wish to express their gratitude and sincere appreciation to the National Natural Science Foundation of China (51778370, 51861165204, 51538007), Natural Science Foundation of Guangdong Province (2017B030311004) and Shenzhen Science and Technology Funding (JCYJ20170818094820689) for financing this research work.

References

1 K. Yu, Q. Shi, M. L. Dunn, T. Wang and H. J. Qi, *Adv. Funct. Mater.*, 2016, **26**, 6098.
2 J. H. Zhu, L. Wei, H. Moahmoud, E. Redaelli, F. Xing and L. Bertolini, *Constr. Build. Mater.*, 2017, **151**, 127.
3 J. H. Zhu, M. N. Su, J. Y. Huang, T. Ueda and F. Xing, *Constr. Build. Mater.*, 2018, **167**, 669.
4 Y. Yuan, Y. Sun, S. Yan, J. Zhao, S. Liu, M. Zhang, X. Zheng and L. Jia, *Nat. Commun.*, 2017, **8**, 14657.
5 J. Palmer, O. R. Ghita, L. Savage and K. E. Evans, *Composites, Part A*, 2009, **40**, 490.
6 S. J. Pickering, *Composites, Part A*, 2006, **37**, 1206.
7 G. Marsh, *Reinf. Plast.*, 2008, **52**, 36.
8 G. Marsh, *Reinf. Plast.*, 2009, **53**(22), 25.
9 J. Jiang, G. Deng, X. Chen, X. Gao, Q. Guo, C. Xu and L. Zhou, *Compos. Sci. Technol.*, 2017, **151**, 243–251.
10 Y. Wang, X. Cui, H. Ge, Y. Yang, Y. Wang, C. Zhang, J. Li, T. Deng, Z. Qin and X. Hou, *ACS Sustainable Chem. Eng.*, 2015, **3**, 3332–3337.
11 W. Nie, J. Liu, W. Liu, J. Wang and T. Tang, *Polym. Degrad. Stab.*, 2015, **111**, 247.
12 J. Li, P. L. Xu, Y. K. Zhu, J. P. Ding, L. X. Xue and Y. Z. Wang, *Green Chem.*, 2012, **14**, 3260.

13 R. Piñero-Hernanz, C. Dodds, J. Hyde, J. García-Serna, M. Poliakoff, E. Lester, M. J. Cocero, S. Kingman, S. Pickering and K. H. Wong, *Composites, Part A*, 2008, **39**, 454.
14 R. Piñero-Hernanz, J. García-Serna, C. Dodds, J. Hyde, M. Poliakoff, M. J. Cocero, S. Kingman, S. Pickering and E. Lester, *J. Supercrit. Fluids*, 2008, **46**, 83.
15 A. Loppinetserani, C. Aymonier and F. Cansell, *J. Chem. Technol. Biotechnol., Biotechnol.*, 2010, **85**, 583.
16 G. Jiang, S. J. Pickering, G. S. Walker, K. H. Wong and C. D. Rudd, *Appl. Surf. Sci.*, 2008, **254**, 2588.
17 S. J. Pickering, R. M. Kelly, J. R. Kennerley, C. D. Rudd and N. J. Fenwick, *Compos. Sci. Technol.*, 2000, **60**, 509.
18 H. L. H. Yip, S. J. Pickering and C. D. Rudd, *Plast., Rubber Compos.*, 2002, **31**, 278.
19 H. Sun, G. Guo, S. A. Memon, W. Xu, Q. Zhang, J. H. Zhu and F. Xing, *Composites, Part A*, 2015, **78**, 10.
20 A. Katsaounis, *J. Appl. Electrochem.*, 2010, **40**, 885.
21 J. S. Association, n.d.
22 G. Jiang, S. J. Pickering, G. S. Walker, K. H. Wong and C. D. Rudd, *Appl. Surf. Sci.*, 2008, **254**, 2588.
23 M. Li, C. Feng, Z. Zhang, X. Lei, R. Chen and Y. Yang, *J. Hazard. Mater.*, 2009, **171**, 724–730.
24 K. Rajeshwar and J. G. Ibanez, *Environmental Electrochemistry: Fundamentals and Applications in Pollution Sensors and Abatement*, Academic Press, 1997.
25 Z. Jin, Z. Zhang and L. Meng, *Mater. Chem. Phys.*, 2006, **97**, 167.
26 N. S. Zhu, H. Y. Li, F. X. Wang and Y. S. Dai, *Appl. Mech. Mater.*, 2014, **490–491**, 298.
27 K. Sawaki, S. Asai, K. Watanabe, T. Sugo and K. Saito, *Membrane*, 2008, **33**, 32.
28 T. Takahagi and A. Ishitani, *Carbon*, 1984, **22**, 43.
29 S. K. Ryu, B. J. Park and S. J. Park, *J. Colloid Interface Sci.*, 1999, **215**, 167.
30 S. Zhang, X. Y. Li and J. P. Chen, *J. Colloid Interface Sci.*, 2010, **343**, 232.
31 S. H. Han, H. J. Oh, H. C. Lee and S. S. Kim, *Composites, Part B*, 2013, **45**, 172.
32 K. Giannadakis, M. Szpieg and J. Varna, *Exp. Mech.*, 2011, **51**, 767.